



Effect of Proof Loading on the Fatigue Life of Mooring Lines

Fábio José C. da Silva Filho¹, Michele A.L. Martins¹, Evilly Raquel H. da Silveira¹, Eduardo N. Lages¹, Mauro C. Oliveira²

¹*Scientific Computing and Visualization Laboratory, Federal University of Alagoas
Cidade Universitária, 57072-970, Maceió/AL, Brazil*

fabio.filho@ctec.ufal.br, micheleagra@lccv.ufal.br, evilly.silveira@ctec.ufal.br, enl@lccv.ufal.br

²*CENPES/PETROBRAS*

Av. Horácio Macedo, 950 - Cidade Universitária da Universidade Federal do Rio de Janeiro, 21941-915, Rio de Janeiro/RJ, Brazil

mauro@petrobras.com.br

Abstract. The oil and gas industry, crucial for the global economy, is influenced by offshore exploration and, consequently, by the use of mooring lines for deepwater production. This study investigates the effects of proof load variation on the fatigue behavior of mooring lines, directly impacting the efficiency and safety of these operations. A comparative analysis of four mooring models subjected to tensile and bending loads using finite element analysis is conducted. Numerical models were developed in ABAQUS® software, varying proof load magnitudes of 65%, 70%, 75%, and 80% of the Minimum Breaking Load (MBL). The models simulate proof loading, unloading, operational tension, and out-of-plane bending (OPB) steps. The investigation assesses stress concentration factors (SCFs) and OPB stiffness to understand how varying proof loads affect mooring line fatigue. Results reveal distinct locking and sliding phases, with higher proof loads leading to greater OPB moments during the locking phase. These analyses highlight the necessity of accurately evaluating OPB stiffness under different loading conditions to predict and mitigate fatigue failures. The study emphasizes that SCFs for tension-tension (TT) and OPB modes vary significantly with proof load magnitude, influencing stress at hotspots and impacting the fatigue life of mooring lines.

Keywords: out-of-plane bending, in-plane bending, fatigue, proof loading, mooring lines.

1 Introduction

The oil and gas industry is responsible for numerous technological advancements and directly influences the global economy. Offshore exploration contributes to its expansion, which allows gas and oil production in deep waters. In this context, mooring lines are crucial elements that enable the activities of floating platforms in such conditions, ensuring their stability and positioning.

Throughout their operational life, mooring lines are subjected to cyclic loads influenced by environmental loads, such as waves, currents, and wind. Traditional standards used to consider only tensile forces to evaluate fatigue damage in mooring lines, ignoring the effects of combined stresses [1]. Recent advancements in engineering practices have underscored the limitations of traditional fatigue analysis, especially when mooring lines are subjected to high tensile loads along with substantial variations in top angles at the fairlead. Cases of premature failures in mooring lines of operational units due to fatigue have highlighted the considerable influence of Out-of-Plane Bending (OPB) and In-Plane Bending (IPB) effects [2]. Therefore, this topic emerged as a significant area of study for researchers. However, developing new fatigue assessment models that consider the combined effects of stresses, including out-of-plane bending and in-plane bending, has been challenging due to

the high number of parameters involved and the variability of anchoring system configurations.

OPB and IPB phenomena originate from the mooring manufacturing process, where a proof load is applied that causes plastic deformation of the contact surface between the links, which restricts the relative rotation between subsequent links [3]. The proof load consists of a tensile load applied to the links that promotes residual compressive stresses, increasing fatigue resistance [4]. Various standards recommend applying a proof load in the range of 65% to 80% of the Minimum Breaking Load (MBL) [5].

Furthermore, various studies and projects aim to understand the effects of varying proof load magnitudes and the interferences in parameters related to the fatigue life of moorings. A study [6] intended to compare the effects of fatigue life for high and normal proof load intensities. Berthelsen [7] studied the influence of proof load and other factors on the out-of-plane bending phenomenon.

In this context, this study aims to conduct a comparative analysis of four mooring models subjected to tensile and bending loads using finite element analysis (FEA). The analysis examines different proof load magnitudes, investigating parameters such as OPB angle variation, OPB moment, and stress concentration factors.

2 Overall analysis procedure

Guidelines provided by the classification society and certification organization Bureau Veritas (BV-NI604) [8] outline the procedure for fatigue damage assessment, considering combined stresses. This methodology is divided into four phases: development of fatigue sea states, development of interlink stiffness and stress concentration factors, global response analysis and local modeling, and stress calculation and cycle counting. Such guidelines provide the equations to calculate the stress concentration factors (SCF) to determine the TT and OPB stresses at the respective hotspots, as shown in the following equations:

$$SCF_{TT} = \frac{\pi d^2 \Delta \sigma_{TT}}{2 \Delta T} \quad (1)$$

$$SCF_{OPB} = \frac{\pi d^3 \Delta \sigma_{OPB}}{16 \Delta M_{OPB}} \quad (2)$$

where SCF_{TT} , SCF_{OPB} and SCF_{IPB} are the Stress Concentration Factors for TT, OPB and IPB respective modes, respectively; $\Delta \sigma_{TT}$ and $\Delta \sigma_{OPB}$ represent the effective stress for each corresponding mode. ΔT denotes the tensile load acting on the line, ΔM_{OPB} is the OPB moment d is the diameter of chain link. In the last phase, the total combined stress ($\sigma_{combined}$) time series at each OPB hotspot can be estimated from eq. (3). This equation is obtained by applying the appropriate stress concentration factors to the nominal stress components ($\sigma_{mode,nom}$). Due to the two symmetry planes of the chain link and the phase difference between the loads, the combination of stresses and the fatigue analysis must be conducted at each of the four locations (Fig.1).

$$\sigma_{combined} = SCF_{TT} \cdot \sigma_{TT,nom} \pm SCF_{OPB} \cdot \sigma_{OPB,nom} \pm SCF_{IPB} \cdot \sigma_{IPB,nom} \quad (3)$$

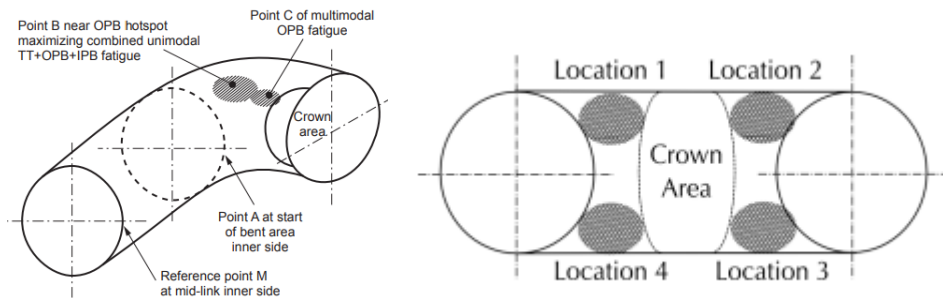


Figure 1. Hotspots on a chain link for combined fatigue (BV NI 604, 2014).

To finalize the fatigue damage assessment, a rainflow cycle counting procedure is applied to the overall stress time series to develop the stress range histogram for each sea state. Subsequently, the long-term stress range histogram is generated by combining these individual sea state histograms, weighted by their respective probabilities of occurrence.

Since the TT, OPB, and IPB hotspot stresses are located in different parts of the chain link (Fig.1), the location

of fatigue failure can vary depending on the magnitude of each loading. The OPB hotspot is located in an area with a slow stress gradient. Therefore, different locations within the OPB hotspot area can be defined. The point that maximizes the additional effects of TT loading and the IPB effects in this area should be considered as the fatigue failure location, rather than the point of maximum OPB, to maximize the combined stress. Hotspots are generally identified as: pure TT hotspot or hotspot A; uniaxial OPB hotspot maximizing the effects of TT, OPB, and IPB, referred to as hotspot B; and multiaxial OPB hotspot with multiaxial effects closer to the contact area, identified as hotspot C.

3 Methodology and Study Models

Following a methodological study on the OPB phenomenon and the normative recommendations of BV-NI604 [8], four finite element models were developed in the ABAQUS® software. These models, composed of three links at different proof loading magnitudes, represent the stages of proof loading, unloading, operational tension, and out-of-plane bending. Post-processing techniques were incorporated to evaluate parameters such as stress concentration factors and OPB stiffness.

The numerical models consist of three links (a complete link in the center subjected to OPB and two half-links at the ends, one fixed link and the other for load application, considering symmetry in the XY plane), with a diameter of 107 mm. The type of element used for the links was C3D8I. A thin membrane was also modeled on the surface of the link with M3D4 elements to evaluate the stress. The loads were applied at a reference point that had its movements linked to the load application section of the loading link. For this study, five boundary conditions were used, which are defined below:

- BC-1: Symmetry-type condition applied to the faces of the links in the XY plane. Boundary condition applied to all steps.
- BC-2: Symmetry-type condition applied to the faces of the fixed link in the Y direction. Boundary condition applied to all steps.
- BC-3: Condition of type Displacement/Rotation, applied to "RP-1". Constraint of displacements in the X and Z directions and rotations in the X, Y and Z directions in initial steps. In the bending step, this condition is modified, considering constraints of displacements in the Z direction and rotations in the X and Y.
- BC-4: Condition of type Displacement/Rotation, applied to "RP-1". Constraint of a rotation of 2° in the Z direction. Boundary condition applied in the bending step.
- BC-5: Condition of type Displacement/Rotation, applied to the faces of the fixed link. Constraint of displacements in the X and Z directions. Boundary condition applied in the bending step.

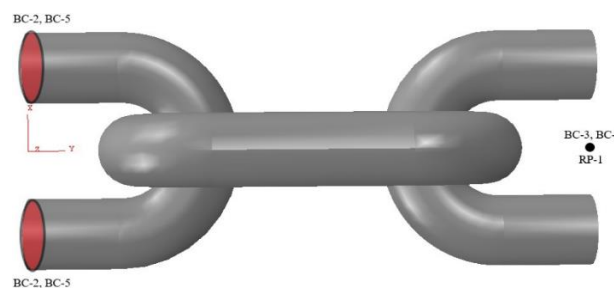


Figure 2. Boundary Conditions of the study model.

The contact properties considered were normal and tangential. For the normal contact, "Hard" - Contact was employed for the activation pressure and the contact imposition method was designated as Penalty formulation. Regarding the tangential contact, the friction approach used was the Penalty type, and the coefficient of friction selected was 0.3. The load magnitudes for the four models vary between 65% and 80% of the Minimum Breaking Load (MBL), specifically at 65% ($5.8814E+06$ N), 70% ($6.3338E+06$ N), 75% ($6.7862E+06$ N), and 80% ($7.2386E+06$ N), considering an R3 steel material grade. The Minimum Breaking Load was calculated using the formulations provided by DNVGL (Eq. 4) [9], i.e.,

$$MBL = 0.0223 \cdot d^2 \cdot (44 - 0.08 \cdot d) \tag{4}$$

where MBL refers to the Minimum Breaking Load in kN for the R3 steel material category and d represents the diameter of the mooring link in mm. The analysis also considered an operational load of 2.2653E+06 N and a rotational angle of 0° – 2.00° range.

4 Results and discussion

Figure 3a presents the relationship between the prescribed angle at the load application point and the OPB angle, while Fig. 3b shows the relationship between the OPB angle and the OPB moment. The results indicate an increasing phase of the OPB moment, representing the locking phase between the links. After this phase, a sliding phase between the links is observed, reaching the OPB moment limit. Additionally, it can be noted that the greater the applied proof load, the higher the OPB moment during a significant portion of the locking phase.

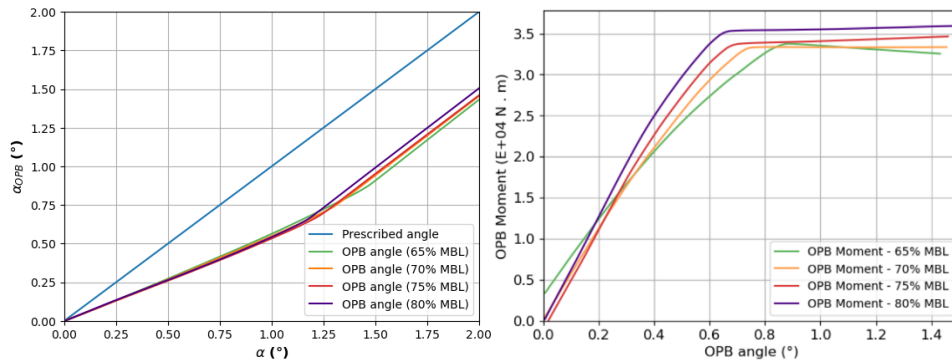


Figure 3. (a) OPB angle versus the prescribed rotation at RP-1; (b) OPB angle versus OPB Moment.

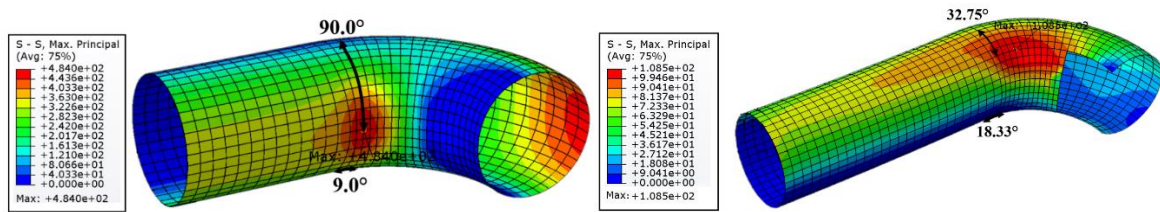


Figure 4. Angular location of hotspots for the TT and OPB stress fields of the 65% MBL model, respectively.

Table 2. TT stress and SCF values for the four models

Nodes (Hotspot)	Angular Location	σ_{nom}	σ_{EF}	SCF
65% MBL	{9.0°, 90.0°}	1.2596E+8 Pa	4.8649E+8 Pa	3.86
70% MBL	{9.0°, 90.0°}	1.2596E+8 Pa	5.0429E+8 Pa	4.0
75% MBL	{9.0°, 90.0°}	1.2596E+8 Pa	3.8733E+8 Pa	3.07
80% MBL	{13.5°, 90.0°}	1.2596E+8 Pa	3.3339E+8 Pa	2.65

Table 3. OPB stress and SCF values for the four models to an OPB angle of 0.37°

Nodes (Hotspot)	Angular Location	σ_{nom}	σ_{EF}	SCF
65% MBL	{18.33°, 32.75°}	8.1053E+7 Pa	1.0905E+8 Pa	1.35
70% MBL	{49.39°, 50.53°}	8.3050E+7 Pa	1.1265E+8 Pa	1.36
75% MBL	{9.32°, 52.09°}	8.8104E+7 Pa	1.8248E+8 Pa	2.07
80% MBL	{9.32°, 52.09°}	9.6016E+7 Pa	2.2140E+8 Pa	2.31

The angles between the links for the different study cases exhibit very similar values until the start of the sliding phase, where these values of OPB angles are smaller as the proof load increases, and then they begin to diverge. In the sliding phase, the higher the applied load test, the greater the developed OPB angles. This results from the amplified magnitude of the OPB moment, due to the expanded contact area between the links.

Tables 2 and 3, respectively, evaluate the location of the hotspot stress and the stress concentration factors for pure TT at the end of the tension step, and for pure OPB at an OPB angle of 0.37° (during the locking phase). In some cases, the stress concentration factors exhibited significantly different values, highlighting the influence of the magnitude of the proof load on this parameter. The location of the hotspot region for pure TT in the study cases was found to be more localized, whereas the region for pure OPB was more extensive. The tables also indicate the angular position of the post-processed nodes, which are stress hotspots: the first angle is defined from the beginning of the elbow, while the second angle is defined from the median plane of the link (Fig. 4).

5 Conclusions

The investigation into OPB stiffness under varying proof loads reveals a crucial understanding of the fatigue behavior of mooring lines. The study identifies distinct phases of locking and sliding between the links. The results indicate that higher proof loads lead to greater OPB moments during a significant portion of the locking phase. Additionally, the angles between the links show very similar values until the start of the sliding phase, after which these values diverge with smaller OPB angles for higher proof loads. In the sliding phase, higher applied loads result in greater developed OPB angles due to the increased magnitude of the OPB moment. These findings underscore the need to accurately evaluate OPB stiffness in different loading conditions to mitigate fatigue.

In conclusion, this study underscores the importance of understanding the stress concentration factors (SCFs) for different proof loads in the fatigue damage assessment of mooring lines. The results indicate that SCFs for TT and OPB modes can vary significantly with the magnitude of the applied load. This variability influences the effective stress at the hotspots, impacting the overall fatigue life of the mooring lines. Notably, current standards suggest unique SCF values for hotspots across different modes without considering variations in proof loads, highlighting a critical gap that this study addresses.

Acknowledgements. The authors acknowledge PETROBRAS and CNPq for the financial support.

Authorship statement. The authors hereby confirm that they are the sole liable persons responsible for the authorship of this work, and that all material that has been herein included as part of the present paper is either the property (and authorship) of the authors, or has the permission of the owners to be included here.

References

- [1] L. Rampi, A. Bignonnet, C. Cunff, F. Bourgin and P. Vargas. "Chain Out of Plane Bending (OPB) Fatigue Joint Industry Project (JIP) FEA Results and Multiaxiality Study Results". ASME 2016 35th International Conference on Ocean, Offshore and Arctic Engineering, Busan, South Korea, 2016.
- [2] C. Melis, P. Jean and P.M. Vargas. "Out-of-plane bending testing of chain links". Proceedings of the ASME 2005 24th International Conference on Offshore Mechanics and Arctic Engineering, 2005.
- [3] L. Rampi, F. Dewi, M. Francois, A. Gerthoffert and P. Vargas. "Chain Out of Plane Bending (OPB) Fatigue Joint Industry Project (JIP) Static Test Program and OPB Interlink Stiffness". ASME 2016 35th International Conference on Ocean, Offshore and Arctic Engineering, Busan, South Korea, 2016.
- [4] G. Shoup, S. Tipton, J. Sorem. "The Influence of Proof Loading on the Fatigue Life of Anchor Chain". Offshore Technology Conference, Houston, 1992.
- [5] Denton GN. "An assessment of proof load effect on the fatigue life of mooring chain for floating offshore installations". Mooring Integrity Joint Industry Project Phase 2, 2017.
- [6] Noble Denton & Associates. "Corrosion Fatigue Testing of 76mm Grade R3 & R4 Studless Mooring Chain". Report No. H5787\NDAI\MJW, 2002.
- [7] K. Berthelsen. "Out of plane bending of mooring chains - finite element analysis of a 7-link model", Master's Thesis, Norwegian University of Science and Technology, 2017.
- [8] Bureau Veritas. "Fatigue of Top Chain of Mooring Lines Due to In-plane and Out-of-plane Bendings". Guidance Note NI 604 DT R00 E, 2014.
- [9] DNV GL. Offshore standard – offshore mooring chain (DNVGL-OS-E302), Edition July 2018, 2018.